Proceedings of the Estonian Academy of Sciences,
2015, **64**, 3S, 449–456
doi: 10.3176/proc.2015.3S.16
Available online at www.eap.ee/proceedings

NONLINEAR WAVES

Transition of breakup modes for a liquid jet in a static electric field

Takao Yoshinaga* and Takasumi Iwai

Osaka University, Osaka, Toyonaka 560-8531, Japan

Received 17 March 2015, accepted 30 June 2015, available online 28 August 2015

Abstract. We analytically investigate breakup phenomena of a viscous liquid column jet closely placed in a concentric sheath on which a static electric field is imposed. Taking account of a surrounding electric field of the jet, long wave nonlinear equations of the jet radius, velocity, and electric surface charge density are derived. These equations are numerically solved for the initial-boundary condition that a semi-spherical jet initially emanates from a nozzle exit. It is shown that there exist three types of breakup modes – jetting, spraying, and spinning – depending upon the parameters Λ (electric force/fluid inertial force) and Pe (convective current/conductive current). Then, critical curves are found in the $\Lambda - \mathrm{Pe}$ parameter space, across which the mode is transferred from the jetting to the spinning through the spraying with the increase of Λ and/or the decrease of Pe. In the transition from jetting to spraying mode, the produced drop size gradually decreases with the increase of Λ for larger Pe. On the other hand, there is a range of Λ where the drop size discontinuously decreases with increasing Λ for smaller Pe, which may lead to producing a satellite drop.

Key words: liquid jet, electric field, instability, electro-spraying, electro-spinning.

1. INTRODUCTION

Techniques of electro-spraying and -spinning are available to produce fine liquid drops and thin fibres of submicron order [1]. These phenomena are based on fluid motions in a static electric field known in the electrohydrodynamics (EHD) [2]. Since the pioneering work by Lord Rayleigh [3] in 19th century, many investigators have made experimental and analytical works in the field of the EHD. It is widely known in experiments for a jet emanating from a nozzle that the jet forms a conical surface near the nozzle which is now referred to as the Taylor cone [4], and a series of fine liquid drops or a thin thread is produced from a tip of the cone when the electric field strength is sufficiently large [5]. Whereas such experimental investigations have been actively performed, theoretical works are not sufficient and have been only focused on the followings [6–8]: (i) relations between flow rates and carried electric currents on a steady semi-infinite jet under an axial electric field and (ii) temporal instabilities and breakup profiles of the jet on a uniform infinite jet without any influence of the axial electric field. In practice, however, the jet is not only unsteady but also finite in length with or without any axial electric field.

Recently, the present authors [9] examined breakup of an unsteady jet emanating from a nozzle under an axial electric field and show that the jet breaks up by producing a liquid drop or a thin thread depending upon the strength of the electric field and conductivity of the liquid. However, for simplicity, they assumed that the axial electric field is constant on the surface of the jet, in spite that the surrounding electric field is variable due to electric charges on the deformable jet surface. Therefore, in the present analysis, we

* Corresponding author, yoshinag@me.es.osaka-u.ac.jp

consider the influence of surrounding electric field on the breakup process, when the jet is closely placed in a concentric cylindrical sheath on which an electric field is imposed. Using reduced nonlinear equations under a long wave approximation, the breakup modes of the jet, emanating from a nozzle, are examined and existing regions of the modes and produced drop sizes are revealed in the governing parameter space.

2. FORMULATION

We consider the liquid jet in a static electric field as shown in Fig. 1, where the jet is viscous and slightly conductive and placed inside the concentric sheath on which the constant axial electric field E_w is imposed. According to the leaky dielectric model [10], we assume that the charge stays only on the jet surface and, therefore, there is no charge inside and outside the jet except for the surface. In the present analysis, for simplicity, we do not consider any motion of surrounding gas and influence of the gravitational force. Assuming the $z-r$ axisymmetric coordinate system, the jet radius is prescribed by $r = h(z,t)$ and the sheath radius is by L (constant). The liquid density is denoted by ρ, the velocity by $\boldsymbol{u} = (u(z,r,t), v(z,r,t))$, and the surface charge density by $\sigma_e(z,t)$, while the electric fields outside and inside the jet by $\boldsymbol{E}^{(o)} = (E_z^{(o)}(z,r,t), E_r^{(o)}(z,r,t))$, and $\boldsymbol{E}^{(i)} = (E_z^{(i)}(z,r,t), E_r^{(i)}(z,r,t))$, respectively.

Then, the basic equations consist of the continuity and momentum equations of the jet for $0 \le r < h$:

$$\nabla \cdot \boldsymbol{u} = 0, \tag{1a}$$

$$\rho(\partial \boldsymbol{u}/\partial t + \boldsymbol{u} \cdot \nabla \boldsymbol{u}) = \nabla \cdot D, \tag{1b}$$

where the stress tensor $D = -pI + \mu(\nabla \boldsymbol{u} + (\nabla \boldsymbol{u})^T)$ with viscosity μ and unit matrix I is introduced, while the electric field is continuous and irrotational in both inside ($0 \le r < h$) and outside ($h < r < L$) the jet because of no electric charge and no magnetic field (the magnetic field acts passively in a slightly conducting fluid even if it exists):

$$\nabla \cdot \boldsymbol{E}^{(o)} = \nabla \cdot \boldsymbol{E}^{(i)} = 0, \tag{2a}$$

$$\nabla \times \boldsymbol{E}^{(o)} = \nabla \times \boldsymbol{E}^{(i)} = 0. \tag{2b}$$

Besides, on the surface, the surface charge density is governed by [2]

$$\partial \sigma_e/\partial t + \boldsymbol{u}_n \cdot \nabla_n \sigma_s + \nabla_s \cdot (\sigma_s \boldsymbol{u}_s) + \sigma_s(\boldsymbol{n} \cdot \boldsymbol{u})\kappa = -[(K\boldsymbol{E} + \sigma_e \boldsymbol{u}) \cdot \boldsymbol{n}]_{(i)}^{(o)}, \tag{3}$$

where $[(\cdot)]_{(i)}^{(o)} = (\cdot)_{(o)} - (\cdot)_{(i)}$ denotes the jump in the quantity $(\cdot)$ across the interface and the curvature $\kappa = h^{-1}[1 + (\partial h/\partial z)^2]^{-1/2} - (\partial^2 h/\partial z^2)[1 + (\partial h/\partial z)^2]^{-3/2}$. In the above representation, K denotes the electric conductivity, $\boldsymbol{u}_n = \boldsymbol{n}(\boldsymbol{n} \cdot \boldsymbol{u})$, $\boldsymbol{u}_s = \boldsymbol{t}(\boldsymbol{t} \cdot \boldsymbol{u})$, $\nabla_n = \boldsymbol{n}(\boldsymbol{n} \cdot \nabla)$, and $\nabla_s = \nabla - \nabla_n$, where $\boldsymbol{n}$ and $\boldsymbol{t}$ are the normal and tangential unit vectors on the surface, respectively.

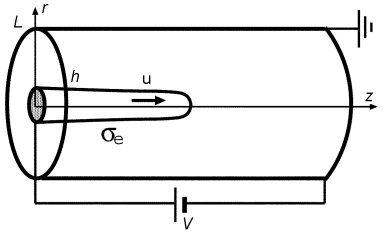

Fig. 1. Schematic of a liquid jet in a sheath of cylindrical wall under a static electric field.

On the other hand, the kinematical boundary conditions at $r = h$ consist of

$$\partial F/\partial t + \boldsymbol{u}\cdot\nabla F = 0, \tag{4a}$$

$$\boldsymbol{E}^{(o)}\cdot\boldsymbol{t} = \boldsymbol{E}^{(i)}\cdot\boldsymbol{t}, \tag{4b}$$

$$\varepsilon^{(o)}\boldsymbol{E}^{(o)}\cdot\boldsymbol{n} - \varepsilon^{(i)}\boldsymbol{E}^{(i)}\cdot\boldsymbol{n} = \sigma_e, \tag{4c}$$

where $F \equiv r - h = 0$, while $\varepsilon^{(i)}$ and $\varepsilon^{(o)}$ are the dielectric constants inside and outside the jet. The dynamical conditions are given in the normal and tangential components, respectively,

$$[\boldsymbol{n}\cdot D\cdot\boldsymbol{n} + \boldsymbol{n}\cdot T\cdot\boldsymbol{n}]_{(i)}^{(o)} = \gamma\kappa, \tag{5a}$$

$$[\boldsymbol{t}\cdot D\cdot\boldsymbol{n} + \boldsymbol{t}\cdot T\cdot\boldsymbol{n}]_{(i)}^{(o)} = 0. \tag{5b}$$

In the above, the surface tension γ and the Maxwell stress tensor $T = \varepsilon[\boldsymbol{EE} - (1/2)\boldsymbol{I}\boldsymbol{E}\cdot\boldsymbol{E}]$ are introduced, where $\boldsymbol{EE}$ and $\boldsymbol{E}\cdot\boldsymbol{E}$ denote the dyadic and inner products, respectively.

Assuming the jet to be sufficiently thin compared with wave length of deformation, we can introduce the following long wave approximation (slender jet approximation) for the pressure p and the axial components u and $E_z^{(i)}$, where we have considered that the derivatives of these variables with respect to r should vanish on the axis:

$$p = p_0(z,t) + r^2 p_1(z,t) + \cdots, \tag{6a}$$

$$u = u_0(z,t) + r^2 u_1(z,t) + \cdots, \tag{6b}$$

$$E_z^{(i)} = E_{z0}^{(i)}(z,t) + r^2 E_{z1}^{(i)}(z,t) + \cdots, \tag{6c}$$

which lead to the leading terms of the radial components v and $E_r^{(i)}$ from Eqs (1a) and (2a)

$$v = -(r/2)(\partial u_0/\partial z) - (r^3/4)(\partial u_1/\partial z) - \cdots, \tag{7a}$$

$$E_r^{(i)} = -(r/2)(\partial E_{z0}^{(i)}/\partial z) - (r^3/4)(\partial E_{z1}^{(i)}/\partial z)\cdots. \tag{7b}$$

On the other hand, from Eqs (2) for the outer electric field $\boldsymbol{E}^{(o)}$, the electrostatic potential ϕ, given as $\boldsymbol{E}^{(o)} = -\nabla\phi$ satisfies, $\nabla^2\phi = 0$ or

$$(\partial^2\phi/\partial z^2) + r^{-1}(\partial/\partial r)(r\partial\phi/\partial r) = 0. \tag{8}$$

Since the concentric cylindrical sheath is close to the jet surface, we can assume that the wave length of variation in ϕ is much larger in z than in r. Then we introduce a new strained coordinate $\xi = \lambda^{1/2}z$ instead of z and expanding ϕ as $\phi = \phi_1 + \lambda\phi_2 + \cdots$ in terms of a small parameter λ. Making use of these new coordinate and expansion into Eq. (8), we have the following equations in the lowest and second orders of λ:

$$O(1) : r^{-1}(\partial/\partial r)(r\partial\phi_1/\partial r) = 0, \tag{9a}$$

$$O(\lambda) : r^{-1}(\partial/\partial r)(r\partial\phi_2/\partial r) + \partial^2\phi_1/\partial\xi^2 = 0. \tag{9b}$$

Introducing the unknown function $f(\xi,t)$ and using the boundary condition $\phi_1 = \phi_w$ and $\phi_2 = 0$ at $r = L$, we have the following solutions: $\phi_1 = \phi_w + f\ln(L/r)$ and $\phi_2 = -(1/4)(\partial^2 f/\partial\xi^2)[r^2(\ln(L/r)+1) - (\ln r/\ln L)L^2]$. These solutions are combined and written in terms of the original variable z as follows:

$$\phi = \phi_w + f\ln(L/r) - (r^2/4)f''[1+\ln(L/r)] + (f''/4)(\ln r/\ln L)L^2, \tag{10}$$

where $'$ denotes $\partial/\partial z$ and $(\partial/\partial\xi) = \lambda^{-1/2}(\partial/\partial z)$ has been used. As a result, the components of the outer electric field are given as

$$E_z^{(o)} = E_w - f'\ln(L/r) + (f'''/4)[r^2(1+\ln(L/r)) - (\ln r/\ln L)L^2], \tag{11a}$$

$$E_r^{(o)} = f/r + f''[r/4 + (r/2)\ln(L/r) - L^2/(4r\ln L)]. \tag{11b}$$

Substituting the representations for the inner and outer electric fields in Eqs (6c), (7b), and (11) into (4b) and (4c) at $r = h$, we have

$$E_w - \ln(L/h)[(f' - (h^2/4)f'''] + (f'''/4)[(h^2 - (\ln h/\ln L)L^2] + h'\Big[(f/h) + (h/4)f''[1+2\ln(L/h)] - (f''/4h)(L^2/\ln L)\Big] = E_{z0}^{(i)} - (h^2/4)(\partial^2 E_{z0}^{(i)}/\partial z^2) - (h/2)h'(\partial E_{z0}^{(i)}/\partial z), \tag{12a}$$

$$\sqrt{1+h'^2}\sigma_e = \varepsilon^{(o)}\Big[-h'E_w + h'f'\ln(L/h) + (f/h) + (h/4)f''[1+2\ln(L/h)] + (L^2/4\ln L)[h'f'''\ln h - (f''/h)]\Big] + \varepsilon^{(i)}[h'E_{z0}^{(i)} + (h/2)(\partial E_{z0}^{(i)}/\partial z)], \tag{12b}$$

where higher order terms than $O(h^2)$ are neglected, leaving $\ln h$ and $\ln L$ to be of $O(1)$. Multiplying (12a) by h' and substituting into (12b) to eliminate f', we have the following representation for f when considered up to $O(h^2)$:

$$f = (h\sigma_e/\varepsilon^{(o)}) - \beta h h' E_{z0}^{(i)} - (\beta+1)(h^2/2)(\partial E_{z0}^{(i)}/\partial z) - (f''/4)[2h^2\ln(L/h) + h^2 + L^2/\ln L], \tag{13}$$

where $\beta = \varepsilon^{(i)}/\varepsilon^{(o)} - 1$. For the cylindrical sheath, which is close to the thin jet, we may assume that L is also small enough to be of $O(h)$ and, therefore, we may neglect higher order terms than $O(h)$ and $O(L)$ keeping both $\ln h$ and $\ln L$ to be of $O(1)$. Then we have from Eqs (12a) and (13)

$$E_z^{(i)} = E_w + (h'\sigma_e/\varepsilon^{(o)}) - [(h\sigma_e)'/\varepsilon^{(o)}]\ln(L/h) + O(h^2), \tag{14}$$

where we have used $E_z^{(i)} = E_{z0}^{(i)} + O(h^2)$. Using the above representation and noting that $r \sim L \sim h$ and E_w is constant, we have from (11)

$$E_z^{(o)} = E_w - [(h\sigma_e)'/\varepsilon^{(o)}]\ln(L/r) + O(h^2), \tag{15a}$$

$$E_r^{(o)} = r^{-1}[(h\sigma_e/\varepsilon^{(o)}) - hh'\beta E_w] + O(h^2). \tag{15b}$$

The inner electric field $E_r^{(i)}$ is obtained from (7b) with the help of (14) as

$$E_r^{(i)} = -(r/2\varepsilon^{(o)})[h'\sigma_e - (h\sigma_e)'\ln(L/h)]' + O(h^3), \tag{16}$$

which is found to vanish when we consider up to $O(h)$, since $r \sim h$.

Consequently, as far as we consider up to $O(h)$, the electric field on the jet surface $r = h$ for constant E_w is written as

$$E_z^{(o)} = -[(h\sigma_e)'\varepsilon^{(o)}]\ln(L/h) + E_w, \tag{17a}$$

$$E_z^{(i)} = (h'\sigma_e/\varepsilon^{(o)}) - [(h\sigma_e)'/\varepsilon^{(o)}]\ln(L/h) + E_w, \tag{17b}$$

$$E_r^{(o)} = (\sigma_e/\varepsilon^{(o)}) - h'\beta E_w, \tag{17c}$$

$$E_r^{(i)} = 0. \tag{17d}$$

Similar representations to the above electric field on the jet surface have been obtained by rather rough estimations. When the self induction due to the surface charge is not considered [11,12], the same representation as $E_z^{(i)}$ is obtained for $E_z^{(o)}$ by assuming $E_z^{(o)} \simeq E_z^{(i)}$, while $E_r^{(o)} = \sigma_e/\varepsilon^{(o)}$ by assuming $\varepsilon^{(i)}E_n^{(i)} \ll \varepsilon^{(o)}E_n^{(o)}$. On the other hand, when the self-induction is considered [12,13], the term of the axial electric field is obtained on the surface, though the coefficients are difficult to determine since the effect of the surface charge along the whole domain of jet should be integrated. In the present case that the coaxial cylindrical sheath is close to the jet, it is enough to consider the local condition of the electric field and the representations (17) are appropriate and used in the following analysis.

Using the above representations (17), we next derive the jet equations. Substituting the expansion of v in Eq. (7a) into the kinematical condition (4a), we have in the lowest order of the approximation

$$\partial h/\partial t = -u_0(\partial h/\partial z) - (h/2)(\partial u_0/\partial z). \tag{18}$$

Making use of the expansions p, u, and v in Eqs (6a), (6b), and (7a) into the z component of Eq. (1b), we have in the lowest order of the approximation

$$\partial u_0/\partial t + u_0(\partial u_0/\partial z) = \rho^{-1}(\partial p_0/\partial z) + (\mu/\rho)(4u_1 + \partial^2 u_0/\partial z^2). \tag{19}$$

Using the same expansions together with Eq. (17) into the normal component of the dynamical boundary condition in Eq. (5a), we have

$$p_0 = p_a - \mu(\partial u_0/\partial z) - (\varepsilon^{(o)}E_w^2/2)\beta - (\sigma_e^2/2\varepsilon^{(o)}) + \gamma\kappa, \tag{20}$$

with the atmospheric pressure p_a, while we have from the tangential component in Eq. (5b)

$$\begin{aligned} u_1 = {} & (3h'/2h)(\partial u_0/\partial z) + (1/4)(\partial^2 u_0/\partial z^2) + (2h\mu)^{-1}\Big[\sigma_e E_w + h'(\sigma_e^2/\varepsilon^{(o)}) \\ & - (\sigma_e/\varepsilon^{(o)})(h\sigma_e)'\ln(L/h) - \varepsilon^{(o)}h'\beta E_w^2\Big]. \end{aligned} \tag{21}$$

Substituting Eqs (20) and (21) into Eq. (19) we finally obtain the momentum equation

$$\begin{aligned} \partial u_0/\partial t + u_0(\partial u_0/\partial z) = {} & -(\gamma/\rho)(\partial\kappa/\partial z) + 3\mu(\rho h^2)^{-1}(\partial/\partial z)(h^2\partial u_0/\partial z) \\ & + \rho^{-1}\Big[(\sigma_e/\varepsilon^{(o)})(\partial\sigma_e/\partial z) + (2E_w\sigma_e/h) + (2h'/h)(\sigma_e^2/\varepsilon^{(o)}) - 2\sigma_e(h\sigma_e)'(h\sigma_e\varepsilon^{(o)})^{-1}\ln(L/h)\Big], \end{aligned} \tag{22}$$

where we note the terms with β do not appear in the above equation within the present order of the approximation. Making use of expansions (6) and (7) into Eq. (3), we have in the lowest order approximation

$$\partial\sigma_e/\partial t + u_0(\partial\sigma_e/\partial z) + (\sigma_e/2)(\partial u_0/\partial z) = -K^{(i)}E_w(\partial h/\partial z), \tag{23}$$

where we have neglected the small terms $K^{(o)}$ and $\sigma_e\boldsymbol{u}\cdot\boldsymbol{n}$ on the surface.

Choosing the characteristic length, velocity, and time as the undisturbed jet radius a, speed U, and a/U and taking the characteristic dielectric constant, conductivity, and strength of the electric field as $\varepsilon^{(o)}$, $K^{(i)}$ and E_0, Eqs (18), (22), and (23) can be written in the following normalized forms:

$$\partial h/\partial t + u(\partial h/\partial z) = -(h/2)(\partial u/\partial z), \tag{24a}$$

$$\begin{aligned} \partial u/\partial t + u(\partial u/\partial z) = {} & -\mathrm{Wb}^{-1}(\partial\kappa/\partial z) + (3/\mathrm{Re})h^{-2}(\partial/\partial z)[h^2(\partial u/\partial z)] \\ & + \Lambda\Big[\sigma_e(\partial\sigma_e/\partial z) + (2E_w\sigma_e/h) + (2\sigma_e^2/h)(\partial h/\partial z) - (2\sigma_e/h)(\partial h\sigma_e/\partial z)\ln(L/h)\Big], \end{aligned} \tag{24b}$$

$$\partial\sigma_e/\partial t + u(\partial\sigma_e/\partial z) = -(\sigma_e/2)(\partial u/\partial z) - (E_w/\mathrm{Pe})(\partial h/\partial z), \tag{24c}$$

where the suffix 0 on u have been dropped. In the above, we have introduced the non-dimensional parameters $\mathrm{Wb} = \rho aU^2/\gamma$ (Weber number), $\mathrm{Re} = \rho aU/\mu$ (Reynolds number), $\mathrm{Pe} = \varepsilon^{(o)}U/(aK^{(i)})$ (Electric Peclet number), and $\Lambda = \varepsilon^{(o)}E_0^2/(\rho U^2)$ (Taylor number($\equiv \varepsilon^{(o)}aE_0^2/\gamma$) /Wb). In particular, Pe means the ratio of the convective current to the conductive current ($\varepsilon^{(o)}UE_0 2\pi a/(\pi a^2 KE_0)$), while Λ the ratio of the electrostatic force to the fluid inertial force ($(\varepsilon^{(o)}E_0)E_0/(\rho U^2)$). It should be noted that the third and fourth terms in the parenthesis of Λ in Eq. (24b) disappear in the previous work [9].

3. RESULTS

In the analysis, we adopt the following initial-boundary condition: $h(z,0) = \sqrt{1-z^2}$, $u(z,0) = 1$ and $\sigma_e(z,0) = 1$ and $h(0,t) = u(0,t) = \sigma_e(0,t) = 1$. The calculations are carried out by using the CIP (Cubic Interpolated Pseudo-particle) method for the advection phase and the time splitting method for the non-advection phase [9,14]. In the CIP method both dependent variables and their spatial derivatives in the advection phase are interpolated with cubic polynomials in each grid. In the calculations, numerical grid sizes are taken to be $\Delta t = 0.0001$ and $\Delta z = 0.1$ in order to retain the numerical accuracy within the relative error of 1.5% in the volume ratio. In the present analysis, the parameters Wb $= 10$, Re $= 100$, $E_w = 1$, and $L = 2$ are fixed, while Pe and Λ are chosen as the control parameters.

Numerical results show that there exist three different breakup modes in Λ–Pe parameter space as shown in Fig. 2, where typical breakup profiles are exemplified in the subwindows of each mode. In the jetting mode (a) which appears for smaller Λ and larger Pe, the jet produces a large liquid drop at the top and breaks up by pinching off. In this mode the surface tension is dominant in the smaller electric force and less conductivity of the liquid. In the spray mode (b), however, we can find that the drop size is drastically reduced to a microdrop at the tip of the cone because of the suppression of the surface tension as Λ increases. And, in the spinning mode (c) which appears for larger Λ and smaller Pe, the microdrop disappears and the jet makes a cone shape profile near the nozzle exit and subsequently becomes thinner to the downward without any liquid drop. In this mode the electric force becomes superior to the surface tension for more conductive liquid.

Finally, in the transition from jetting to spraying mode, Fig. 3 shows the average drop size $D_{\rm ave}(= 2(3V/4\pi)^{1/3}$ for the volume V of the drop), where the drop size varies continuously for larger Pe ≥ 40, while discontinuously for smaller Pe ≤ 30. Figure 4 shows how such discontinuous changes of the drop size appear, where the breakup profiles are given near the critical values of Λ for Pe $= 10$. From this figure we may predict that the resulting produced drop size is still large in (a) for $\Lambda = 0.07$, since the jet breaks up not near the tip at $z \sim 92$ but at the smaller $z \sim 72$ and the resulting fragmentation of the jet would become a large spherical drop. However, in (b) for $\Lambda = 0.08$, the jet breaks up near the tip at $z \sim 88$ to produce a small drop. Since the jet would disintegrate at smaller $z \sim 65$ after that, a large drop is produced. As a result, a smaller drop is followed by a larger drop, that is, a satellite drop is produced in this case.

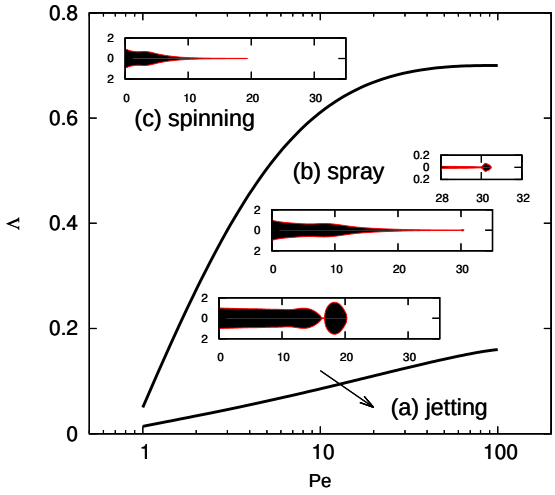

Fig. 2. Critical curves discriminating the jetting, spray, and spinning modes in (Λ, Pe) space, where typical breakup profiles in these modes are shown in the subwindows for which the ordinates mean r and the abscissas z.

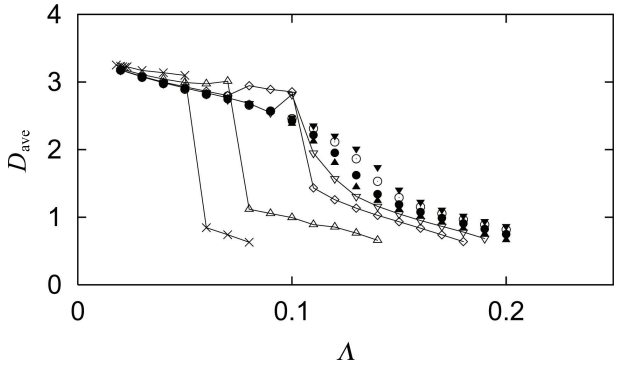

Fig. 3. Produced liquid drop sizes $D_{\rm ave}$ for different values of Λ and Pe, where Pe =500, 100, 50, and 40 are, respectively, denoted by $\blacktriangle, \circ, \bullet$ and $\blacktriangle$, while Pe =30, 20, 10, and 5 are denoted by $\triangledown, \Diamond, \triangledown$ and $\times$.

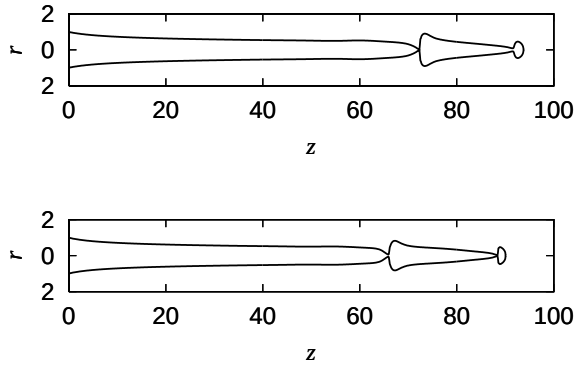

Fig. 4. Breakup profiles near the critical curves, where Pe = 10 and $\Lambda = 0.07$ in (a), while Pe = 10 and $\Lambda = 0.08$ in (b).

4. CONCLUSIONS

Finally we summarize our results as follows. Under the long wave approximation for the jet and electric field, the reduced nonlinear equations are derived when the axial electric field is imposed on the concentric sheath. The critical curves separating regions of the jetting, spraying, and spinning modes are obtained in the $\Lambda -$ Pe parameter space, across which the breakup changes from the jetting to spinning mode through the spraying mode with the increase of Λ and/or the decrease of Pe. In the transition from the jetting to spraying mode, the produced drop size decreases continuously with the increase of Λ for larger Pe, while the size is discontinuously reduced for smaller Pe which leads to producing a satellite drop.

ACKNOWLEDGEMENT

This work has been partially supported by the Grant-in-Aid for Science Research from the Ministry of Education, Culture, Sports, Science, and Technology of Japan (No. 21560177).

REFERENCES

1. Li, D. and Xia, Y. Electrospinning of nanofibers: reinventing the wheel?. *Adv. Mater.*, 2004, **16**, 1151–1170.
2. Castellanos, A. *Electrohydrodynamics* (Castellanos, A., ed.). Springer, Wien, 1998.

3. Lord Rayleigh. On the equilibrium of liquid conducting masses charged with electricity. *Phil. Mag.*, 1882, **14**, 184–186.
4. Taylor, G. I. Electrically driven jets. *P. Roy. Soc. Lond. A Mat.*, 1969, **313**, 453–475.
5. Cloupeau, M. and Prunet-Foch, B. Electrohydrodynamic spraying functioning modes: critical review. *J. Aerosol Sci.*, 1994, **25**, 1021–1036.
6. Fernández de la Mora, J. The fluid dynamics of Taylor cones. *Annu. Rev. Fluid Mech.*, 2007, **39**, 217–243.
7. Barrero, A. and Loscertales, I. G. Micro- and nanoparticles via capillary flows. *Annu. Rev. Fluid Mech.*, 2007, **39**, 89–106.
8. Collins, T. T., Jones, J. J., Harris, M. T., Basaran, O. A. Electrohydrodynamic tip streaming and emission of charged drops from liquid cones. *Nat. Phys.*, 2008, **4**, 149–154.
9. Yoshinaga, T. and Iwai, T. Breakup of a liquid column jet in a static electric field. *Theoretical and Applies Mechanics Japan*, 2013, **62**, 219–226.
10. Saville, D. A. Electrohydrodynamics: the Taylor–Melcher leaky dielectric model. *Annu. Rev. Fluid Mech.*, 1997, **29**, 27–64.
11. Melcher, J. R. and Warren, E. P. Electrohydrodynamics of a current-carrying semi-insulating jet. *J. Fluid Mech.*, 1971, **47**, 127–143.
12. Ganan-Calvo, A. M. On the theory of electrohydrodynamically driven capillary jets. *J. Fluid Mech.*, 1997, **335**, 165–188.
13. Hohman, M. M., Shin, M., Rutledge, G., and Brenner, M. P. Electrospinning and electrically forced jets. I. Stability theory. *Phys. Fluids*, 2001, **13**, 2201–2220.
14. Yabe, T. and Aoki, T. A universal solver for hyperbolic equations by cubic-polynomial interpolation. I. One-dimensional solver. *Comput. Phys. Commun.*, 1991, **66**, 219–232.

Staatilises elektriväljas asuva vedelikujoa lagunemisviiside teisenemine

Takao Yoshinaga ja Takasumi Iwai

On vaadeldud viskoosse vedeliku juga, mis asub kontsentrilises kestas ja millele mõjub staatiline elektriväli. On uuritud vedelikujoa lagunemisprotsessi. Joa raadiuse, kiiruse ja elektrilise pinnalaengu tiheduse jaoks on tuletatud mittelineaarsed pikkade lainete võrrandid, mis võtavad arvesse juga ümbritseva elektrivälja mõju. Saadud võrrandid on lahendatud numbriliselt, eeldades, et düüsist väljub algselt poolsfääriline juga. Lagunemisel võib juga kas keerduda, muutuda tilkadeks või pihustuda. On näidatud, milliste juga ja elektrivälja iseloomustavate parameetrite väärtuste korral läheb üks lagunemisviis üle teiseks.